Colloids and Surfaces B: Biointerfaces 163 (2018) 146–154

Contents lists available at ScienceDirect

Colloids and Surfaces B: Biointerfaces

journal homepage: www.elsevier.com/locate/colsurfb

Anhydrous reverse micelle lecithin nanoparticles/PLGA composite microspheres for long-term protein delivery with reduced initial burst

Longkai Chen[a,b,1], Liling Mei[a,b,1], Disang Feng[b], Di Huang[b,2], Xin Tong[b], Xin Pan[b], Chune Zhu[a,*], Chuanbin Wu[a,b]

[a] Institute for Biomedical and Pharmaceutical Sciences, Guangdong University of Technology, Guangzhou 510006, China
[b] School of Pharmaceutical Sciences, Sun Yat-sen University, Guangzhou 510006, China

ARTICLE INFO

Article history:
Received 21 September 2017
Received in revised form
29 November 2017
Accepted 20 December 2017
Available online 21 December 2017

Keywords:
Microspheres
Lecithin nanoparticles
Poly (lactic-co-glycolic) acid
Macromolecular protein drugs
Long-term drug delivery

ABSTRACT

To address the issue of initial burst release from poly (lactic-co-glycolic) acid (PLGA) microspheres prepared by water-in-oil-in-water (W/O/W) double emulsion technique, PLGA composite microspheres containing anhydrous reverse micelle (ARM) lecithin nanoparticles were developed by a modified solid-in-oil-in-water (S/O/W) technique. Bovine serum albumin (BSA) loaded ARM lecithin nanoparticles, which were obtained by initial self-assembly and subsequent lipid inversion of the lecithin vesicles, were then encapsulated into PLGA matrix by the S/O/W technique to form composite microspheres. *In vitro* release study indicated that BSA was slowly released from the PLGA composite microspheres over 60 days with a reduced initial burst (11.42 ± 2.17% within 24 h). The potential mechanism of reduced initial burst and protein protection using this drug delivery system was analyzed through observing the degradation process of carriers and fitting drug release data with various kinetic models. The secondary structure of encapsulated BSA was well maintained through the steric barrier effect of ARM lecithin nanoparticles, which avoided exposure of proteins to the organic solvent during the preparation procedure. In addition, the PLGA composite microspheres exhibited superior biocompatibility without notable cytotoxicity. These results suggested that ARM lecithin nanoparticles/PLGA composite microspheres could be a promising platform for long-term protein delivery with a reduced initial burst.

© 2017 Elsevier B.V. All rights reserved.

1. Introduction

With the rapid development of proteomics and genomics, a number of biopharmaceuticals including peptides and proteins have been recently discovered and applied in the clinic setting due to their excellent bioactivity and strong specificity [1,2]. However, protein molecules are generally fragile and susceptible to external conditions such as acidic/alkali medium, high temperature/pressure and ultraviolet irradiation, which may lead to rapid degradation of proteins. Moreover, protein drugs usually have short half-lives, which presents as a main obstruction in the maintenance of the effective therapeutic concentration of drugs [3].

Most peptide and protein drugs in the market are administered parenterally and frequent injections are generally necessary for the treatment of chronic diseases, which may result in poor compliance and various complications [4]. Therefore, development of long-term protein delivery systems is urgently required to reduce the injection frequency thereby improving patients' compliance [5,6].

It has been reported that polymeric microspheres are promising drug carriers, which allow sustained drug release over a long period of time and protect labile biomolecules by encapsulating them into the polymer matrix [7]. Among commonly used polymers, PLGA is one of the excipients approved by the Food and Drug Administration for human use in therapeutic devices. Although PLGA microspheres have been intensively investigated in the medical and pharmaceutical fields due to great biocompatibility and biodegradability [8–12], effectively encapsulating protein drugs into the polymer matrix and minimizing the initial burst still remain challenging. The W/O/W double emulsion technique is commonly used to formulate PLGA microspheres due to its simple and rapid preparation procedure [13]. Nonetheless, the hydrophilic protein drugs could easily diffuse to the external water phase during the fabrication process and distribute over the surface of microspheres

* Corresponding author
E-mail address: chunezhu1108@gdut.edu.cn (C. Zhu).
[1] First Co-authors.
[2] Current affiliation: Buchanan Ocular Therapeutics Unit, Department of Ophthalmology, New Zealand National Eye Centre, Faculty of Medical and Health Sciences, The University of Auckland, Private Bag 92019, Auckland 1142, New Zealand.

https://doi.org/10.1016/j.colsurfb.2017.12.040
0927-7765/© 2017 Elsevier B.V. All rights reserved.

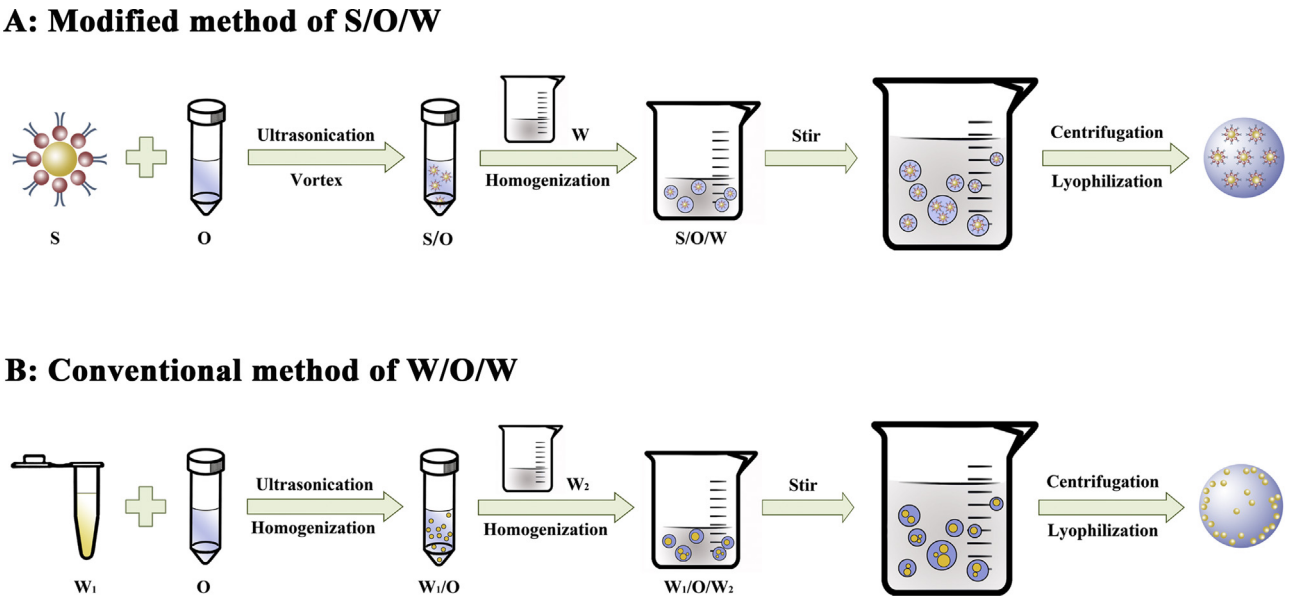

Fig. 1. The schematic illustration of S/O/W method (A) and conventional W/O/W method (B). The larger ball (light yellow) without tails and the smaller balls (light red) with tails in the ARM lecithin nanoparticles (S) indicate BSA and lecithin, respectively. (For interpretation of the references to colour in this figure legend, the reader is referred to the web version of this article.)

with weak-affinity interactions. The protein loaded PLGA microspheres prepared by W/O/W method therefore generally exhibit a remarkable initial burst, which could rise potential risks due to overdose in the initial period and inefficient drug release thereafter [14]. In addition, the conventional W/O/W technique may lead to low encapsulation efficiency of highly water-soluble proteins and inactivation of biopharmaceuticals due to inevitable exposure to organic solvents and water-air interfaces during the preparation process, which could also result in inefficient treatment.

Promisingly, encapsulating the protein drug into composite microspheres might be an effective strategy for the controlled drug release and subsequent efficacy of these bioactive agents [15–17]. This present work aimed to develop ARM lecithin nanoparticles/PLGA composite microspheres by a modified S/O/W method to reduce the initial burst and protect bioactivity of biopharmaceuticals through initially encapsulating protein drugs into ARM lecithin nanoparticles. Physicochemical characteristics of ARM lecithin nanoparticles and microspheres prepared by both S/O/W and W/O/W methods were evaluated, including surface and cross-sectional morphology, *in vitro* drug release, carrier degradation, protein bioactivity, and cytotoxicity. Furthermore, the potential mechanism of reduced initial burst and protein protection using this drug delivery system was analyzed to provide some highlights for the design and development of effective biopharmaceutical platform.

2. Materials and methods

2.1. Materials

Bovine serum albumin (BSA Fraction V, purity 99.65%, Mw 66.5 kDa) and poly (vinyl-alcohol) (PVA 1788, Mw 74.9 kDa) were purchased from Aladdin Chemistry Co., Ltd. (Shanghai, China). PLGA (lactic: glycolic acid = 50: 50, Mw 40 kDa) was purchased from Ji'nan Daigang Biology (Ji'nan, China). Purified soybean lecithin (S100) was obtained from Lipoid GmbH (Ludwigshafen, Germany). Trehalose was gained from Weijia Technology Co., Ltd. (Guangzhou, China). Human keratinocyte cell line (HaCaT) was purchased from China Center for Type Culture Collection (Wuhan, China).

2.2. Preparation of ARM lecithin nanoparticles/PLGA composite microspheres by the S/O/W method

The S/O/W fabrication procedure consisted of two steps (Fig. 1A). Firstly, protein drugs were loaded into lecithin nanoparticles. Secondly, the protein loaded lecithin nanoparticles were embedded into PLGA matrix to formulate lecithin nanoparticles/PLGA composite microspheres.

The protein loaded lecithin nanoparticles were prepared by a modified alcohol injection method. Briefly, BSA, as the model protein, was dissolved in deionized water (2 mg/mL) with addition of trehalose as the lyoprotectant to form the aqueous phase, while lecithin was dissolved in tert-butyl alcohol (TBA, 50 mg/mL) to form the organic phase. The organic phase was then added to the aqueous phase dropwise at a volume ratio of 1:4 under stirring at 1300 rpm for 15 min in a water bath at 37.0 ± 0.5 °C. Afterwards, the mixture was snap-frozen using liquid nitrogen and lyophilized to form solid lecithin nanoparticles (S).

The BSA loaded lyophilized lecithin nanoparticles (S) were subsequently dispersed in 4 mL of DCM containing 400 mg PLGA (organic phase, O) using an ultrasonic processor (SB25-12DT, Ningbo Scientz Biotechnology CO., LTD., China) at 50% amplitude and 0.6 s duty cycle for 1 min. The suspension was then poured into 40 mL of PVA solutions (50 mg/mL, external aqueous phase, W) and homogenized at 10,000 rpm for 1 min in an ice bath to form S/O/W emulsions. Subsequently, the emulsions were immediately transferred into 500 mL of NaCl solutions (50 mg/mL) to evaporate DCM and solidify microspheres under stirring for 3 h at 800 rpm at room temperature. The resulting ARM lecithin nanoparticles/PLGA composite microspheres (S/O/W microspheres) were collected by centrifugation (12,000 rpm, 15 min, room temperature), washed three times with deionized water, lyophilized, and preserved at 4 °C for further experiments.

2.3. Preparation of PLGA microspheres by the W/O/W method

BSA was also encapsulated into PLGA microspheres by the conventional W/O/W double emulsion technique as a comparison (Fig. 1B). Briefly, BSA (2 mg/mL) and trehalose were dissolved in deionized water as the internal aqueous phase (W_1) and PLGA

(100 mg/mL) was dissolved in DCM as the organic phase (O). The internal aqueous phase (1 mL) was added into the organic phase (4 mL) under a rapid homogenization mode at 16,000 rpm for 30 s in an ice bath to form W/O primary emulsions, which were then transferred into 40 mL of the external aqueous phase (W_2) containing PVA (50 mg/mL) and homogenized at 10,000 rpm for 1 min in an ice bath to form W/O/W double emulsions. Subsequently, the double emulsions were placed into 500 mL of NaCl solutions (50 mg/mL) to evaporate organic solvents. Finally, the formulated microspheres were collected, washed, lyophilized, and stored following the aforementioned procedure.

2.4. Characterization of the lecithin nanoparticles and PLGA microspheres

The morphology of BSA loaded original lecithin nanoparticles, ARM lecithin nanoparticles, and reconstructed lecithin vesicles were examined by transmission electron microscopy (TEM, JEM-1400, JEOL, Japan). ARM lecithin nanoparticles were obtained by addition of the lyophilized lecithin nanoparticles into DCM, whereas reconstructed lecithin vesicles were formed by dispersion of the lyophilized lecithin nanoparticles into deionized water. Nanoparticle samples were negatively stained with phosphotungstic acid (1 g/mL) for 2 min prior to TEM observation.

The surface and cross-sectional morphology of the microspheres fabricated by both S/O/W and W/O/W methods was investigated using a scanning electronic microscope (SEM, JSM-6330F, JEOL, Japan). To observe the cross-sectional morphology, the microspheres were pretreated by embedding into a mixed agent consisting of gelatin, glycerin, and water (15: 5: 80, w/w) as well as freezing in liquid nitrogen. The frozen microspheres were then sectioned at approximately 5 μm thicknesses at −40 °C using a frozen microtome. For the SEM observation, both the intact and sectioned microspheres were mounted onto a sample stage and coated with a thin layer of gold under vacuum before observation.

The particles size distribution of BSA loaded ARM lecithin nanoparticles and microspheres prepared by S/O/W method was determined using a Malvern Zetasizer Nano ZS90 (Malvern Instruments, UK) and a laser diffraction Malvern Master Sizer 2000 (Malvern Instruments, UK), respectively. The encapsulation efficiency of both S/O/W and W/O/W microspheres was determined by the previously reported extraction method [18].

2.5. In vitro *drug release*

For *in vitro* drug release, microspheres were weighed, suspended in 1 mL of PBS (pH 7.4), and incubated in a shaking water bath at 37.0 ± 0.5 °C at 100 rpm. Samples were centrifuged (12,000 rpm, 15 min, room temperature) at pre-determined time points and the supernatants were completely replaced with fresh medium to maintain sink conditions. The drug concentration in the collected supernatants was detected using a micro-BCA assay kit and cumulative amounts of BSA released from microspheres were calculated.

To analyze the potential drug release mechanisms, the morphology of microspheres prepared by both S/O/W and W/O/W methods at 15, 30, 45 and 60 days after immersion in the drug release medium was observed by SEM.

2.6. Fourier transformation infra-red (FTIR) spectroscopy

A FTIR spectrometer (EQUTNOX 55, Bruker, Germany) was used to investigate the bonding interactions between the proteins and carrier matrices. FTIR spectra of BSA, blank PLGA microspheres, physical mixture of BSA and PLGA, S/O/W microspheres, and W/O/W microspheres were obtained in the range of 400–4000 cm^{-1} by accumulating 64 scans at 2 cm^{-1} spectral resolution. All samples were thoroughly mixed with potassium bromide at a mass ratio of 1: 200 and compressed into disks before examination.

2.7. Circular dichroism (CD) spectroscopy

The bioactivity of encapsulated proteins was measured by far ultraviolet CD spectroscopy (Chirascan, Applied Photophysics Ltd, UK). The BSA extracted from S/O/W and W/O/W microspheres was dissolved in deionized water transferred into a quartz cell with an optical path length of 1.0 mm and detected in the wavelength range of 180–260 nm under a nitrogen atmosphere.

2.8. Cytotoxicity assay

The cytotoxicity of S/O/W and W/O/W microspheres was evaluated in human keratinocyte cells (HaCaT) using a previously reported methyl thiazolyl tetrazolium (MTT) assay [19]. The viability of cells treated with microspheres at the concentrations of 0.25, 0.50, 1.00, 2.00 and 3.00 mg/mL was expressed as the percentage of their absorbance to that of cells without any treatment in the control group.

2.9. Statistical analysis

All studies were performed at least in triplicate and data were expressed as mean ± S.D. Analysis of variance (one-way ANOVA) followed by Tukey's comparison test was performed using the SPSS 19.0 software (SPSS version 19.0; SPSS Inc., Chicago, USA) to determine statistical significance. Difference was considered significant if $p \leq 0.05$.

3. Results and discussion

3.1. Characterization of BSA loaded lecithin nanoparticles

The TEM images of original lipid nanoparticles in aqueous solution, ARM lecithin nanoparticles in DCM, and reconstructed lipid vesicles in aqueous solution were shown in Fig. 2A_{1-3}, respectively. Results indicated that original lipid nanoparticles and ARM lecithin nanoparticles exhibited irregular shapes with a particle size of around 150 nm. Whereas reconstructed lipid vesicles possessed a relatively large particle size of approximately 200 nm. The increase in particle size might be attributed to hydration of the hydrophobic groups in amphiphilic lecithin molecules and subsequent formation of water layers around individual reconstructed lipid vesicle, which was demonstrated by the external dark shadow surrounding the nanoparticles (Fig. 2A_3).

The formation mechanisms of ARM lecithin nanoparticles during the lyophilization process could be explained by the lipid inversion theory [20]. Briefly, original lipid nanoparticles with lipid bilayers were formed by self-assembly of amphiphilic lecithin with a fraction of dissolved protein molecules. The protein molecules were simultaneously dispersed both in the external aqueous phase and internal cavity of lipid vesicles (Fig. 2D_1). Due to solvent evaporation and phase separation during the lyophilization process, anhydrous nuclei consisting of proteins and lyoprotectants were initially formed and the hydrophilic head groups of lecithin subsequently aggregated and assembled onto the surface of both the encapsulated and free anhydrous nuclei in the inner and outer external aqueous phases (Fig. 2D_2). With addition of the organic phase of DCM, hydrophobic tails of lecithin around the anhydrous nuclei spontaneously stretched and dispersed in the organic phase with hydrophilic heads of lecithin absorbing on the surface of anhy-

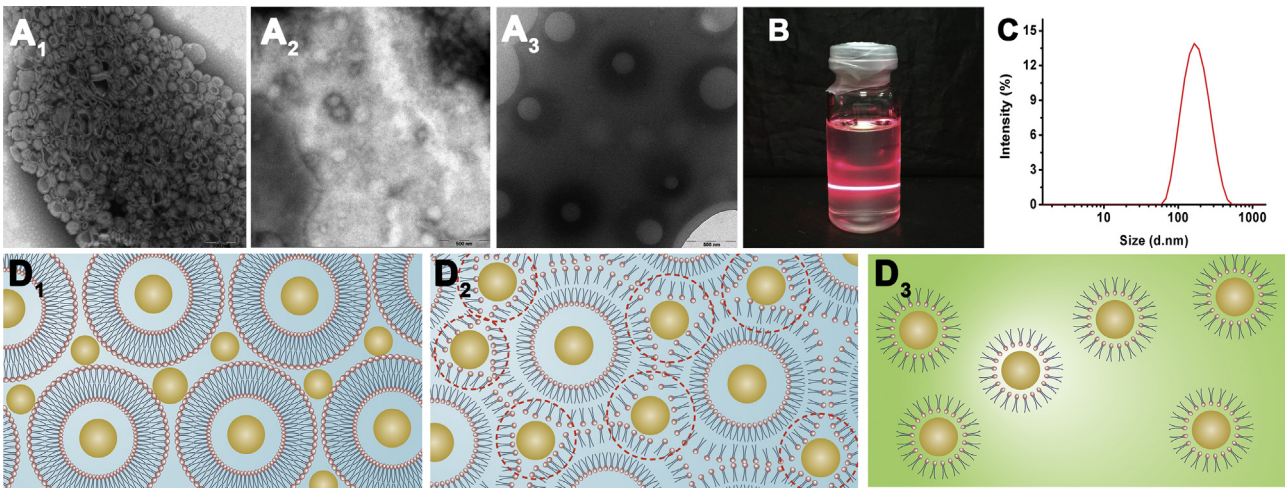

Fig. 2. TEM images of the BSA-loaded original lipid vesicles (A_1), ARM lecithin nanoparticles (A_2) and reconstructed lecithin nanoparticles (A_3); (B) Tyndall effect of BSA-loaded ARM lecithin nanoparticles dispersed in dichloromethane; (C) Size distribution of ARM lecithin nanoparticles; The schematic illustration of the BSA-loaded original lipid vesicles before lyophilization (D_1), lipid inversion of lecithin vesicles during lyophilization (D_2) and ARM lecithin nanoparticles after addition of dichloromethane (D_3). The light blue background in D_1 and D_2 indicates aqueous condition while the light green one in D_3 indicates dichloromethane. The dotted red circles in D_2 depict the formation of BSA-loaded ARM lecithin nanoparticles by lipid inversion. Fig. 2D was modified from our previous publication [20]. (For interpretation of the references to colour in this figure legend, the reader is referred to the web version of this article.)

drous nuclei (Fig. 2D_3) due to the mutual attractions between polar groups of hydrophilic heads of lecithin and protein/lyoprotectant molecules. Afterwards, ARM lecithin nanoparticles were formed, in which the proteins were effectively encapsulated by reverse micelles with the hydrophobic tails facing outwards and homogenously dispersed in the organic phase. The steric barrier effect created by reverse micelles could protect protein molecules against organic solvents [20] and consequently avoid the inactivation of unstable proteins, which is generally induced by exposure to the organic phase during the preparation process of PLGA microspheres via conventional methods.

The Tyndall scattering effect was observed by directing a red laser beam through the suspension of ARM lecithin nanoparticles in DCM, suggesting the colloidal nature of nanoparticle suspensions during the preparation process (Fig. 2B).The average particle size of BSA loaded ARM lecithin nanoparticles was 156.5 ± 3.3 nm with polydispersity index of 0.153 ± 0.013, demonstrating a narrow size distribution (Fig. 2C).

3.2. *Characterization of microspheres*

The surface and cross-sectional morphology of microspheres prepared by both S/O/W and W/O/W techniques was visualized using SEM. The SEM images showed that microspheres formulated via both methods displayed as spheres with smooth surfaces (Fig. 3A_1–B_1). Also, the microspheres prepared by S/O/W method (Fig. 3A_1) exhibited more uniform particle sizes and shapes than that prepared by W/O/W method (Fig. 3B_1). This could be attributed to the superior compatibility of hydrophobic ARM lecithin with PLGA solutions. In contrast, the hydrophilic inter water phase of double emulsions could not be well dispersed in PLGA solutions and non-uniform microparticles were thus formulated. The results were also confirmed by Master Sizer, showing that the S/O/W microspheres exhibited a narrow size distribution with the values of d (0.1), d (0.5), and d (0.9) being 1.479 μm, 2.775 μm, and 4.352 μm, respectively.

Distinguished differences in the inner strutures of microspheres prepared by S/O/W and W/O/W techniques were observed. The S/O/W microspheres showed solid and compact inner structures without formation of cavities or channels (Fig. 3A_2–A_3), whereas large spherical cavities were observed inside the W/O/W microspheres (Fig. 3B_2–B_3). The formation of cavity structures might be due to fusion of emulsion droplets in the internal water phase and subsequent removal of water during solidification of double emulsions and lyophilization of the W/O/W microspheres.

The encapsulation efficiency of BSA in the microspheres prepared by S/O/W and W/O/W methods was $76.02 \pm 5.09\%$ and $68.19 \pm 4.04\%$, respectively. The difference in encapsulation efficiency of microspheres formulated via two techniques could be attributed to the rates of drug migration. Specifically, water-soluble BSA tended to escape from the internal to the external aqueous phase due to the presence of protein concentration gradient during the formation process of W/O/W double emulsions. In contrast, encapsulating BSA into ARM lecithin nanoparticles could effectively avoid drug migration to the external aqueous phase due to the superior compatibility of BSA with the hydrophilic inner phase of ARM lecithin nanoparticles. Therefore, the S/O/W technique achieved higher encapsulation efficiency of protein drugs than the conventional W/O/W method.

3.3. In vitro *drug release behavior and mechanism*

The *in vitro* drug release profiles of microspheres prepared by both S/O/W and W/O/W methods were shown in Fig. 4A. W/O/W microspheres exhibited a significant initial burst with $25.15 \pm 2.43\%$ of drugs released from carriers in the first day, which is a common phenomenon of PLGA microspheres prepared by the conventional W/O/W double emulsion technique, especially for highly hydrophilic protein drugs. After four days with over 50% of drugs rapidly released, a lag phase over one month was observed and followed by a secondary release phase, in which drugs were released at a relatively slow but constant rate. In contrast, S/O/W microspheres achieved sustained and zero-order controlled release with a reduced initial burst ($11.42 \pm 2.17\%$ within 24 h). Particularly, the S/O/W method effectively reduced cumulative amounts of drugs released from microspheres in the first four days by 50% compared to the W/O/W method. The possible explanation is that the S/O/W technique would improve encapsulation efficiency of BSA in the microspheres. During the preparation of the S/O/W microspheres, the protein drugs encapsulated in ARM lecithin nanoparticles were well dispersed in the microspheres due to the superior compatibility of the hydrophobic external phase of ARM

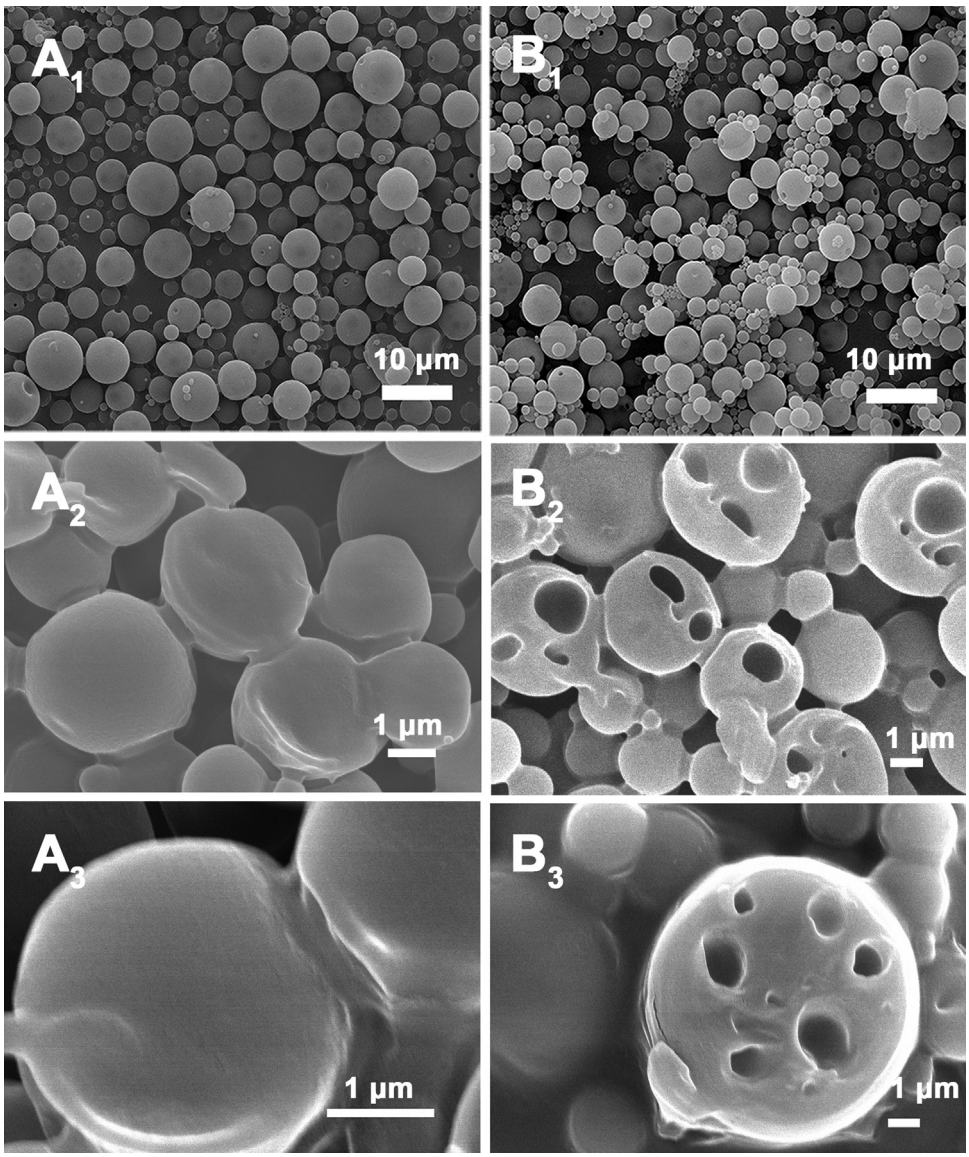

Fig. 3. Surface morphology of the microspheres prepared by S/O/W (A_1) and W/O/W (B_1) methods. Cross section view of the microspheres prepared by S/O/W (A_2, A_3) and W/O/W (B_2, B_3) methods.

with the organic phase of PLGA solutions. The encapsulated BSA was immobilized and maintained in the inner hydrophilic phase of ARM lecithin nanoparticles and thereby achieving sustained and constant drug release from the S/O/W microspheres with a reduced initial burst, which could avoid potential risks of overdose at the initial stage and insufficient drug release at the prolonged stage induced by the initial burst from microspheres prepared by the conventional W/O/W technique.

To explore the drug release mechanisms, the change in surface morphology of microspheres incubated in drug release medium was examined by SEM. After 15 days of immersion in release medium, the morphology of S/O/W microspheres slightly changed with the round-shaped spheres becoming egg-shaped (Fig. 5A). This could be explained that ARM lecithin nanoparticles stabilized PLGA matrix of microspheres through the interactions between the external hydrophobic phase and PLGA, prevented structural collapse of microspheres, and kept their original shapes. Rough surfaces and porous formation were observed after 30 days of immersion (Fig. 5B), while the shape of microspheres further became irregular with hazy outlines due to particle conglutination with each other after 45 days (Fig. 5C). The majority of microspheres collapsed and degraded after 60 days with random-sized and shaped fragments observed (Fig. 5D). The change in morphology of microspheres further confirmed that the sustained and constant drug release behavior of S/O/W microspheres was associated with slow degradation of carriers.

In comparison, W/O/W microspheres exhibited significant changes in morphology with pitted and rough surface examined after 15 days of immersion (Fig. 5E). However, the morphology of W/O/W microspheres hardly changed in the following 15 days (Fig. 5F), demonstrating that W/O/W microspheres did not further degrade over this period of time. This finding was exactly corresponded to the drug release behavior of W/O/W microspheres during the lag phase. Furthermore, W/O/W microspheres showed a crimped surface with porous formation and collapsed into small fragments or particles after 45 (Fig. 5G) and 60 days (Fig. 5H), respectively.

Although encapsulated drugs were completely released from both S/O/W and W/O/W microspheres after approximately two months, different release kinetics were obtained. The drug release

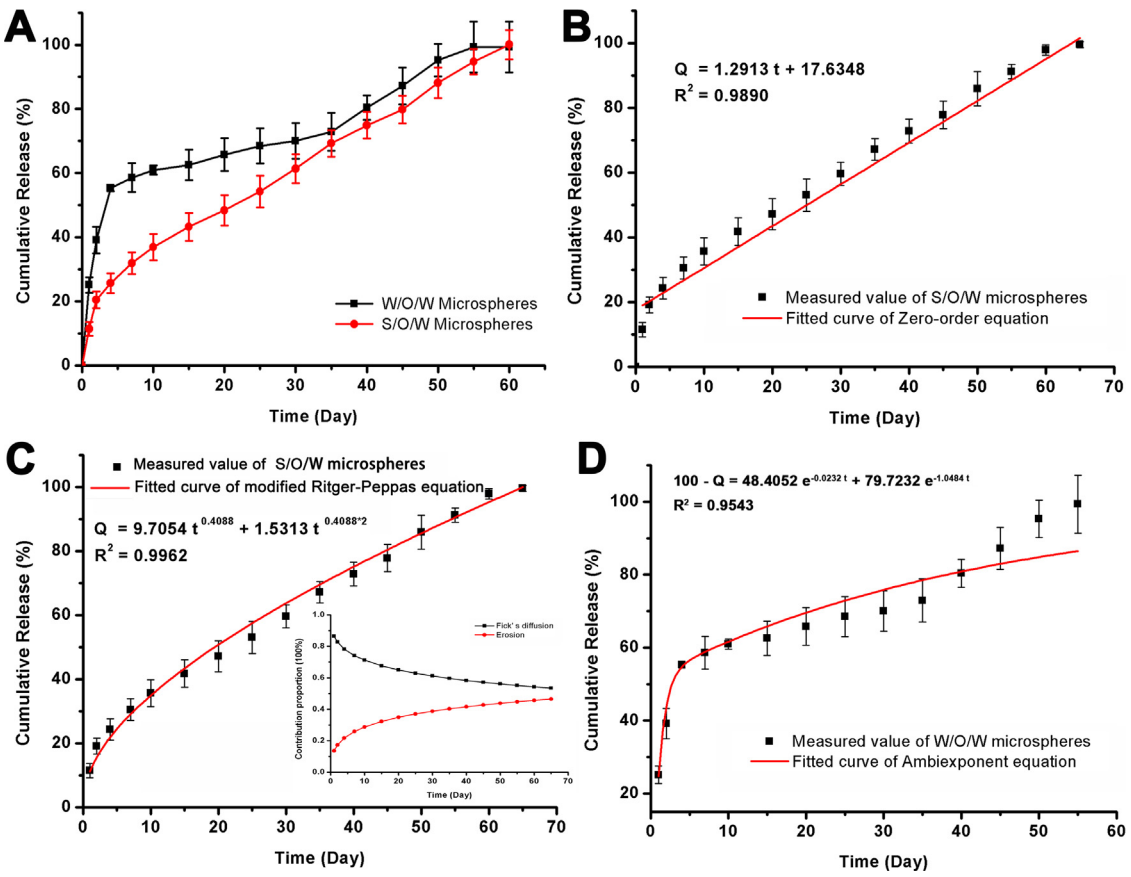

Fig. 4. *In vitro* cumulative drug release profiles of microspheres prepared by both S/O/W and W/O/W methods in PBS (pH 7.4) medium at 37.0 ± 0.5 °C (mean ± S.D., $n = 3$) (A). The fitted curve according to the zero-order controlled release model (B) and the modified Ritger-Peppas model (C) of *in vitro* cumulative release profile for S/O/W microspheres, respectively. The inset demonstrates the contributions of the diffusion-induced and erosion-induced drug release to the cumulative drug release. Fitted curve according to the Ambiexponent model of *in vitro* cumulative release profile for the W/O/W microspheres (D).

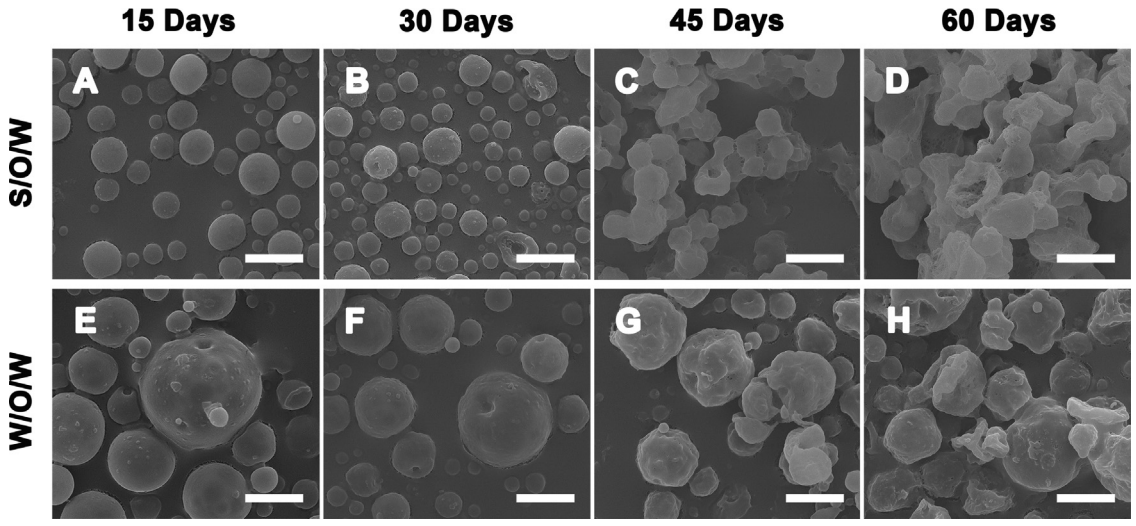

Fig. 5. SEM images of S/O/W and W/O/W microspheres after 15 days (A, E), 30 days (B, F), 45 days (C, G), and 60 days (D, H) of immersion in PBS (pH 7.4) at 37.0 ± 0.5 °C, the scale bars were 5 μm.

profile of S/O/W microspheres was fitted to the zero-order controlled release model (Eq. (1)) and the modified Ritger-Peppas model (Eq. (2)) [21].

$$Q_t = k_1 + a \quad (1)$$

where Q_t indicates the cumulative drug release at time t, k_1 is the constant of drug release rate, and a is a constant.

$$\frac{Q_t}{Q_\infty} = k_1 t^m + k_2 t^{2m} \quad (2)$$

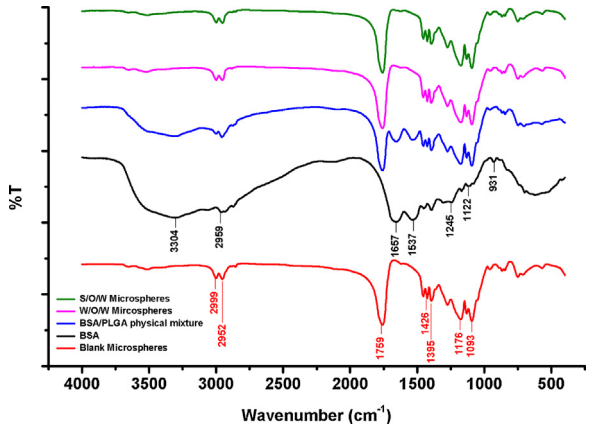

Fig. 6. FTIR spectra of BSA, blank PLGA microspheres, physical mixture of BSA and PLGA, S/O/W microspheres and W/O/W microspheres.

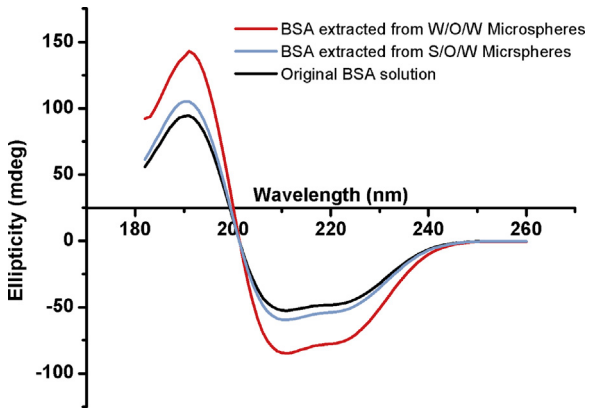

Fig. 7. Far-UV CD spectra of original BSA solution and BSA extracted from S/O/W as well as W/O/W microspheres.

where Q_t and Q_∞ indicate the cumulative drug release at time t and the complete drug release, respectively. The $k_1 t^m$ indicates the diffusion-induced drug release, $k_2 t^{2m}$ indicates erosion-induced drug release, both k_1 and k_2 are constants of drug release rate.

The drug release behavior of S/O/W microspheres followed the zero-order controlled release model with a fitting coefficient of 0.9890 (Fig. 4B), showing a constant drug release rate over the prolonged time period of two months. The drug release mechanisms of S/O/W microspheres could be further explained by the modified Ritger-Peppas model with an extremely high fitting coefficient of 0.9962 (Fig. 4C). The contribution of diffusion- and erosion-induced drug release to cumulative amounts of drugs released from microspheres was mathematically calculated (the inset in Fig. 4C). Results revealed that the drug release behavior of S/O/W microspheres was dominantly dependent on Fick's diffusion laws at the initial stage. Afterwards, the contribution of diffusion-induced drug release gradually reduced, while erosion-induced drug release became the principal mechanism over the later period. The drug release mechanisms were further supported by the SEM results with slow degradation of carriers observed (Fig. 5A–D).

On the other hand, the W/O/W microspheres showed a triphasic drug release behavior consisting of a significant initial burst, a lag stage, and a secondary release phase (Fig. 4A), which was fitted to the Ambiexponent model (Eq. (3)) [22] with a fitting coefficient of 0.9543 (Fig. 4D).

$$100 - Q_t = Ae^{\alpha t} + Be^{\beta t} \quad (3)$$

where Q_t indicates the cumulative drug release at time t. The α phase is the burst region, and the β phase is the sustained region.

The presence of three phases principally depends on the physicochemical properties of encapsulated drugs, drug release kinetics, and PLGA degradation kinetics [23]. The initial burst release could be caused by the rapid escape of drugs deposited either on the surface or in the water channels of microspheres. The highly hydrophilic BSA might easily diffuse to the external phase during the preparation process of W/O/W microspheres, which resulted in the decreased encapsulation efficiency and uneven drug distribution in the microspheres. Due to this, a significant initial burst of BSA released from W/O/W microspheres was observed and the subsequent drug release behavior was also affected accordingly. Another possible explanation is the formation of large cavities or water channels inside the microspheres (Fig. 3B_2–B_3) allowed the rapid flow of release medium through the carrier matrix and thereby increasing the diffusion and release rate of drugs. In addition, the significant initial burst of W/O/W microspheres could also be induced by the dramatic structural collapse of microspheres, which was shown in the SEM images during the first 15 days (Fig. 5E).

In contrast, the modified S/O/W technique would effectively avoid rapid drug migration to the external phase by initially encapsulating BSA into the hydrophilic inner cavity of ARM lecithin nanoparticles. It is worth mentioning that hydrolyzation of PLGA microspheres was also inhibited by lecithin, which stabilized the polymer matrix and enabled the prolonged and sustained drug release with a reduced initial burst.

3.4. FTIR analysis

The interaction between BSA and PLGA polymers was characterized by FTIR spectroscopy. Characteristic bands of proteins were observed in the spectrum of BSA alone (Fig. 6), including the peaks at wavenumbers of 3304 cm^{-1}, 1657 cm^{-1}, 1537 cm^{-1}, and 1245 cm^{-1}, which associated with amide A (υs N—H symmetric vibration), amide I ($\upsilon_{C=O}$ stretching vibration), amide II (δ_{N-H} in-plane bending vibration), and amide III (υ_{C-N} stretching vibration), respectively [24]. The typical peaks of hydrocarbon were obtained in the spectrum of blank PLGA microspheres, including the υ_{C-H} stretching vibration at 2999–2952 cm^{-1} and the δ_{N-H} in-plane bending vibration at 1426–1395 cm^{-1}. It is also believed that the peak at 1759 cm^{-1} corresponded to ester functional groups of the $\upsilon_{C=O}$ stretching band [19].

The characteristic absorption peaks described above were observed in the spectra of the physical mixture of BSA and PLGA, demonstrating that weak or no bonding interactions existed within the components. However, none of the peaks originating from amide A, amide I, and amide II of BSA, was examined in the spectra of S/O/W and W/O/W microspheres, whereas all characteristic absorption signals of PLGA polymer were observed in the spectra of drug loaded microspheres. Our results suggested that BSA was effectively encapsulated into PLGA microspheres using both preparation methods. The more accurate sites for drug distribution in both S/O/W and W/O/W microspheres would be investigated in the future studies by some advanced analytical techniques, such as confocal laser scanning microscope, polarized light microscope, etc [25–28].

3.5. Secondary structure assay of BSA molecules

Lyophilization and emulsion during the preparation process of microspheres might induce dehydration of the BSA-water system and thereby leading to alterations in the secondary structure and subsequent inactivation of protein drugs. The bioactivity of BSA loaded in microspheres was thus determined by analyzing the secondary structure of proteins (i.e. α-helix and β-turn) using far-UV CD spectroscopy [29]. The CD spectrum of original BSA solu-

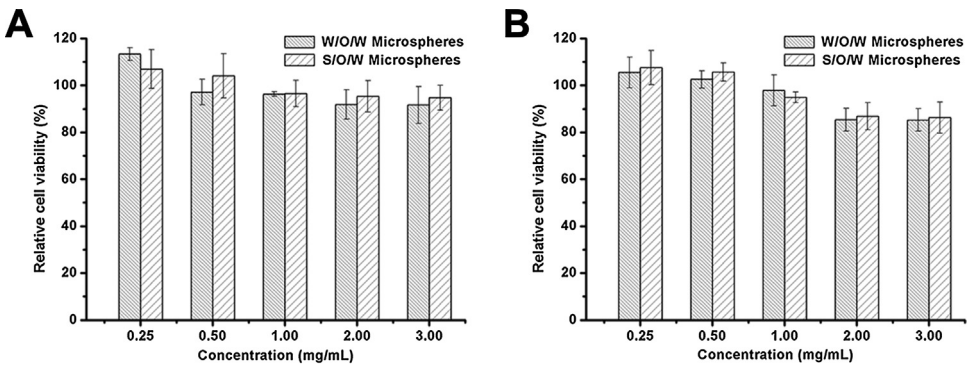

Fig. 8. Cell viabilities of HaCaT cells after 24 h (A) and 48 h (B) of incubation with S/O/W and W/O/W microspheres at various concentrations (mean ± S.D., $n = 5$).

tions (Fig. 7) displayed a single positive dichroic band with a peak around 190 nm and a negative band with double peaks at 209 and 223 nm, which associated with the α-helix structure [30]. The BSA extracted from the microspheres prepared by both techniques showed identical spectra with all characteristic bands presented, suggesting that the secondary structure of proteins encapsulated in the PLGA microspheres was well maintained. Our results indicated that trehalose, as a lyoprotectant, was effective to protect protein drugs against dehydration of the BSA-water system during lyophilization by interacting with proteins instead of water molecules. Hydrophilic trehalose was able to occupy the hydrogen bonding sites between BSA and water molecules when water was gradually evaporated during the lyophilization process and thereby preventing changes in the secondary structure of protein drugs.

Compared to the CD spectrum of original BSA solutions, the ellipticity in the CD spectra of BSA extracted from microspheres slightly shifted with the spectra of W/O/W microspheres showing more significant changes than that of S/O/W microspheres, demonstrating that BSA incorporated in the S/O/W microspheres was stabilized and its secondary structure was kept intact. This could be attributed to the steric barrier effect of ARM lecithin nanoparticles by embedding BSA molecules in the hydrophilic phase of nanoparticles and isolating the encapsulated proteins from the external irritation (Fig. 2D_2). The fragile proteins were thus protected against possible destruction induced by exposure to organic solvents, cross-linking reagents, and oil-water-air interfaces during the formulation process

3.6. Cytotoxicity assay

As shown in Fig. 8, cell viabilities after 24 h and 48 h of incubation with microspheres prepared by both methods were higher than 90% and 85%, respectively, indicating that the microspheres prepared by both S/O/W and W/O/W methods exhibited excellent biocompatibility and biosafety without causing any significant cytotoxicity ($p > .05$).

It is also noted that cell viabilities with addition of both formulations slightly decreased with increasing concentration of microspheres from 0.25 to 3.00 mg/mL as well as prolonging incubation time from 24 h to 48 h. This might be attributed to PLGA degradation and the influence of residual solvent [19]. It is believed that the primary degradation products of PLGA are lactic acid and glycollic acid, which could gradually decrease the pH value of the cell culture medium and thereby reducing the cell viability. Additionally, residual solvents in the microsphere formulations might also contribute to cell death or generation and inhibit the cell viability. Although the organic solvent was effectively removed by lyophilization in this work to reduce cytotoxicity, further studies are required to quantify the residual solvents in the PLGA microspheres prepared by both methods.

4. Conclusion

The ARM lecithin nanoparticles/PLGA composite microspheres with reduced initial burst, was developed by a modified S/O/W technique. The S/O/W microspheres exhibited compact inner structures without formation of any cavities or channels due to the superior compatibility of ARM lecithin nanoparticles with PLGA polymers. The encapsulated protein drugs were well protected through the steric barrier effect of ARM lecithin nanoparticles to isolate proteins from the organic solvent during the preparation process of microspheres. The BSA loaded S/O/W microspheres achieved sustained and zero-order controlled release behavior over two months with no significant initial burst observed, avoiding possible risks induced by the initial rapid drug release from the microspheres prepared by the conventional W/O/W double emulsion method. Furthermore, the S/O/W microspheres exhibited good biocompatibility and biosafety without notable cytotoxicity. In summary, the S/O/W microspheres could be a promising platform for long-term protein delivery system with a reduced initial burst.

Declaration of interest

None.

Conflicts of interest

None.

Acknowledgements

This work was funded by the Science and Technology Plan Projects of Guangdong Province (Grant No. 2015B020232010), the Natural Science Fund Project of Guangdong Province (Grant No. 2016A030312013), the China Postdoctoral Science Foundation (No. 2016M602442) and the Innovative Scientific Research Team Introducing Project of Zhongshan Municipal Government (2015-224).

References

[1] L. Nomcebo Thwala, V. Preat, N. Stefania Csaba, Emerging delivery platforms for mucosal administration of biopharmaceuticals: a critical update on nasal, pulmonary and oral routes, Exp. Opin. Drug Deliv. 14 (2017) 23–36.
[2] M.I. Ugwoke, R.U. Agu, N. Verbeke, R. Kinget, Nasal mucoadhesive drug delivery: background, applications, trends and future perspectives, Adv. Drug Deliv. Rev. 57 (2005) 1640–1665.
[3] R. Visser, G.A. Rico-Llanos, H. Pulkkinen, J. Becerra, Peptides for bone tissue engineering, J. Controll. Release 244 (2016) 122–135.

[4] W. Yuan, Y. Geng, F. Wu, Y. Liu, M. Guo, H. Zhao, T. Jin, Preparation of polysaccharide glassy microparticles with stabilization of proteins, Int. J. Pharm. 366 (2009) 154–159.
[5] M.A. Chowdhury, The controlled release of drugs and bioactive compounds from mesoporous silica nanoparticles, Curr. Drug Deliv. 13 (2016) 839–856.
[6] Z.S. Haidar, R.C. Hamdy, M. Tabrizian, Protein release kinetics for core-shell hybrid nanoparticles based on the layer-by-layer assembly of alginate and chitosan on liposomes, Biomaterials 29 (2008) 1207–1215.
[7] S. Bitencourt Cda, L.B. Silva, P.A. Pereira, G.M. Gelfuso, L.H. Faccioli, Microspheres prepared with different co-polymers of poly(lactic-glycolic acid) (PLGA) or with chitosan cause distinct effects on macrophages, Colloids Surf. B Biointerfaces 136 (2015) 678–686.
[8] T. Qiao, S. Jiang, P. Song, X. Song, Q. Liu, L. Wang, X. Chen, Effect of blending HA-g-PLLA on xanthohumol-loaded PLGA fiber membrane, Colloids Surf. B-Biointerfaces 146 (2016) 221–227.
[9] Z. Liu, Y. Zhu, X. Liu, K.W.K. Yeung, S. Wu, Construction of poly (vinyl alcohol)/poly (lactide-glycolide acid)/vancomycin nanoparticles on titanium for enhancing the surface self-antibacterial activity and cytocompatibility, Colloids Surf. B-Biointerfaces 151 (2017) 165–177.
[10] L. Sun, Z. Liu, L. Wang, D. Cun, H.H.Y. Tong, R. Yan, X. Chen, R. Wang, Y. Zheng, Enhanced topical penetration system exposure and anti-psoriasis activity of two particle-sized, curcumin-loaded PLGA nanoparticles in hydrogel, J. Controll. Release 254 (2017) 44–54.
[11] C. Fornaguera, N. Feiner-Gracia, G. Caldero, M.J. Garcia-Celma, C. Solans, PLGA nanoparticles from nano-emulsion templating as imaging agents: versatile technology to obtain nanoparticles loaded with fluorescent dyes, Colloids Surf. B-Biointerfaces 147 (2016) 201–209.
[12] M.-M. Chen, H. Cao, Y.-Y. Liu, Y. Liu, F.-F. Song, J.-D. Chen, Q.-Q. Zhang, W.-Z. Yang, Sequential delivery of chlorhexidine acetate and bFGF from PLGA-glycol chitosan core-shell microspheres, Colloids Surf. B-Biointerfaces 151 (2017) 189–195.
[13] X. Huang, N. Li, D. Wang, Y. Luo, Z. Wu, Z. Guo, Q. Jin, Z. Liu, Y. Huang, Y. Zhang, C. Wu, Quantitative three-dimensional analysis of poly (lactic-co-glycolic acid) microsphere using hard X-ray nano-tomography revealed correlation between structural parameters and drug burst release, J. Pharm. Biomed. Anal. 112 (2015) 43–49.
[14] A. Sheikh Hasan, A. Sapin, C. Damgé, P. Leroy, M. Socha, P. Maincent, Reduction of the in vivo burst release of insulin-loaded microparticles, J. Drug Deliv. Sci. Technol. 30 (2015) 486–493.
[15] G. Jiang, Y. Wang, R. Zhang, R. Wang, X. Wang, M. Zhang, X. Sun, S. Bao, T. Wang, S. Wang, Preparation of redox-Sensitive shell cross-Linked nanoparticles for controlled release of bioactive agents, ACS Macro Lett. 1 (2012) 489–493.
[16] Y. Wang, G. Jiang, M. Zhang, L. Wang, R. Wang, X. Sun, Facile one-pot preparation of novel shell cross-linked nanocapsules: inverse miniemulsion RAFT polymerization as an alternative approach, Soft Matter 7 (2011) 5348–5352.
[17] D. Liu, G. Jiang, W. Yu, L. Li, Z. Tong, X. Kong, J. Yao, Oral delivery of insulin using CaCO3-based composite nanocarriers with hyaluronic acid coatings, Mater. Lett. 188 (2017) 263–266.
[18] Y.-Y. Yang, T.-S. Chung, N. Ping Ng, Morphology, drug distribution, and in vitro release profiles of biodegradable polymeric microspheres containing protein fabricated by double-emulsion solvent extraction/evaporation method, Biomaterials 22 (2001) 231–241.
[19] C. Zhu, Y. Huang, X. Zhang, L. Mei, X. Pan, G. Li, C. Wu, Comparative studies on exenatide-loaded poly (D,L-lactic-co-glycolic acid) microparticles prepared by a novel ultra-fine particle processing system and spray drying, Colloids Surf. B, Biointerfaces 132 (2015) 103–110.
[20] Z. Huang, H. Wu, B. Yang, L. Chen, Y. Huang, G. Quan, C. Zhu, X. Li, X. Pan, C. Wu, Anhydrous reverse micelle nanoparticles: new strategy to overcome sedimentation instability of peptide-containing pressurized metered-dose inhalers, Drug Deliv. 24 (2017) 527–538.
[21] J. Siepmann, N. Peppas, Modeling of drug release from delivery systems based on hydroxypropyl methylcellulose (HPMC), Adv. Drug Deliv. Rev. 64 (2012) 163–174.
[22] W.J. Hao, T. Xia, Y.Z. Shang, S.H. Xu, H.L. Liu, Characterization and release kinetics of liposomes inserted by pH-responsive bola-polymer, Colloid Polym. Sci. 294 (2016) 1107–1116.
[23] H. Wang, G.X. Zhang, H. Sui, Y.H. Liu, K. Park, W.P. Wang, Comparative studies on the properties of glycyrrhetinic acid-loaded PLGA microparticles prepared by emulsion and template methods, Int. J. Pharm. 496 (2015) 723–731.
[24] J. Depciuch, M. Sowa-Kucma, P. Misztak, B. Szewczyk, G. Nowak, P. Pankiewicz, M. Parlinska-Wojtan, Olfactory bulbectomy-induced changes in phospholipids and protein profiles in the hippocampus and prefrontal cortex of rats. A preliminary study using a FTIR spectroscopy, Pharmacol. Rep. 68 (2015) 521–528.
[25] Y.Y. Yang, T.S. Chung, N.P. Ng, Morphology, drug distribution, and in vitro release profiles of biodegradable polymeric microspheres containing protein fabricated by double-emulsion solvent extraction/evaporation method, Biomaterials 22 (2001) 231–241.
[26] S.E. Varghese, M.K. Fariya, G.S. Rajawat, F. Steiniger, A. Fahr, M.S. Nagarsenker, Lecithin and PLGA-based self-assembled nanocomposite, Lecithmer: preparation, characterization, and pharmacokinetic/pharmacodynamic evaluation, Drug Deliv. Trans. Res. 6 (2016) 342–353.
[27] M. Kastellorizios, N. Tipnis, F. Papadimitrakopoulos, D.J. Burgess, Drug distribution in microspheres enhances their anti-Inflammatory properties in the gottingen minipig, Mol. Pharm. 12 (2015) 3332–3338.
[28] S. Yao, H. Liu, S. Yu, Y. Li, X. Wang, L. Wang, Drug-nanoencapsulated PLGA microspheres prepared by emulsion electrospray with controlled release behavior, Regen. Biomater. 3 (2016) 309–317.
[29] Y. Yue, H.-W. Li, T.-Y. Liu, Y. Wu, Exploring the role of ligand-BSA in the response of BSA-protected gold-nanoclusters to silver (I) Ions by FT-IR and circular dichroism spectra, Vib. Spectrosc. 74 (2014) 137–141.
[30] M. Taha, M.V. Quental, I. Correia, M.G. Freire, J.A.P. Coutinho, Extraction and stability of bovine serum albumin (BSA) using cholinium-based Good's buffers ionic liquids, Process Biochem. 50 (2015) 1158–1166.